

Spin-Wave Doppler Shift by Magnon Drag in Magnetic Insulators

Tao Yu,¹ Chen Wang,² Michael A. Sentef,¹ and Gerrit E. W. Bauer³

¹*Max Planck Institute for the Structure and Dynamics of Matter,
Luruper Chaussee 149, 22761 Hamburg, Germany*

²*Center for Joint Quantum Studies and Department of Physics,
School of Science, Tianjin University, Tianjin 300350, China*

³*Institute for Materials Research & WPI-AIMR & CSRN, Tohoku University, Sendai 980-8577, Japan*

(Dated: January 7, 2022)

The Doppler shift of the quasiparticle dispersion by charge currents is responsible for the critical supercurrents in superconductors and instabilities of the magnetic ground state of metallic ferromagnets. Here we predict an analogous effect in thin films of magnetic insulators in which microwaves emitted by a proximity stripline generate coherent chiral spin currents that cause a Doppler shift in the magnon dispersion. The spin-wave instability is suppressed by magnon-magnon interactions that limit spin currents to values close to but below the threshold for the instability. The spin current limitations by the backaction of magnon currents on the magnetic order should be considered as design parameters in magnonic devices.

Introduction.—Realization of a large spin current is an important pursuit in spintronics. Electrically insulating magnetic films are promising candidate to achieve this goal, allowing low-dissipation information processing by magnons [1–5]. The presently most suitable material to study magnon dynamics is yttrium iron garnet (YIG), a ferrimagnet with high Curie temperature and arguably the lowest damping [6, 7]. Ultrathin YIG films with thicknesses below 10 nm maintain very high magnetic quality [8, 9] and a strongly enhanced Drude-type magnon conductivity [10–12] that should be suitable to carry large spin currents. Recently, large spin currents were observed in ultrathin YIG transistors with DC-current biased Pt gates that inject a large number of nonequilibrium magnons [13–16] into the conducting channel [11, 17].

A Doppler shift of Bogoliubov quasiparticles under an electric current bias is responsible for critical supercurrents in superconductors [18–20]. Similar effect can happen in metallic ferromagnets when using electric currents to excite magnetization dynamics by the spin-transfer torque [21, 22]. The charge current induces a Doppler shift, i.e., a tilt of the spin-wave dispersion of a homogeneous magnetization in momentum space, which could trigger a spin-wave instability [23–25] and modulate the magnetic ground state [26]. These obviously do not apply to magnetic insulators that cannot carry an electric charge current. However, magnetic insulators are also conduits for (magnonic) spin currents that as reported here cause a non-linear Doppler effect by magnon-magnon drag, which also limit the spin current to a material dependent maximum.

In this Letter, we formulate the dynamics of long-wavelength coherent magnons of thin YIG films in the presence of large magnon currents that are pumped by stripline microwaves as depicted in Fig. 1. The polarization-momentum locked AC magnetic field emitted by a microwave stripline [27–29] coherently populates

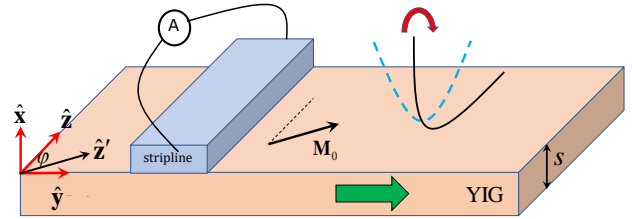


FIG. 1. (Color online) Doppler effect of thin magnetic films driven by pure magnon current. A long stripline along the \hat{z} -direction is illustrated to pump the magnon current (the green thick arrow) in YIG films of thickness s that causes the tilt of magnon dispersion, as shown by the red thick arrow and parabolic bands. The in-plane magnetization is saturated with a relative angle φ to the stripline direction.

magnon states at one side of the stripline with a unidirectional magnon current. We report here that (i) magnon interactions limit the magnitude of this magnon current and the chirality of the pumping, and (ii) an interaction-induced drag effect by the spin current on the magnon dynamics in the form of a magnonic Doppler shift that tilts the spin-wave dispersion into the current direction. The physics of the reported Doppler effect differs strongly from the magnon-drag by phonon [30] or electron [23–25, 31] currents. Its phenomenology is intriguingly similar to an interfacial Dzyaloshinskii-Moriya interaction (DMI) [32–34], but can be tuned by the excitation power. Interaction renders a linear (rather than quadratic) dependence of the excited spin current amplitude at small driving currents. When the drive currents reach a critical value the Doppler shift leads to a dispersion in which the magnon energy vanishes for a finite momentum state, which corresponds to an instability of the ferromagnetic order. However, for stronger drives, higher-order magnon interactions stabilize the magnetization ground state and suppress the spin-wave instability by breaking the chiral-

ity of chiral pumping. We thereby predict a maximum spin current that is close to but (in the absence of a DMI assist) not large enough to cause a spin-wave instability.

Maximal spin current.—We consider an in-plane magnetized YIG film with thickness $s = \mathcal{O}(10)$ nm and saturated magnetization M_s , with surface normal oriented along the $\hat{\mathbf{x}}$ -direction. An in-plane static magnetic field \mathbf{H}_{app} is applied at an angle φ to the stripline $\hat{\mathbf{z}}$ -direction (Fig. 1). The Hamiltonian of the magnetic order reads

$$\hat{H} = \mu_0 \int \left(\frac{\alpha_{\text{ex}}}{2} (\nabla \mathbf{M})^2 - \mathbf{M} \cdot \mathbf{H}_{\text{app}} \right) d\mathbf{r}, \quad (1)$$

where μ_0 is the vacuum permeability, α_{ex} is the exchange stiffness, and \mathbf{M} is the magnetization. We disregard anisotropies [35, 36] because the crystal ones are small in YIG, while the dipolar ones are strongly suppressed in the thin film limit [37, 38]. The exchange length in YIG is $\lambda_{\text{ex}} = 2\pi\sqrt{\alpha_{\text{ex}}} = 109$ nm since $\alpha_{\text{ex}} = 3 \times 10^{-16}$ m² [39, 40]. The magnetization dynamics then obeys a Landau-Lifshitz-Gilbert (LLG) equation

$$\frac{d\mathbf{M}}{dt} = -\mu_0\gamma\mathbf{M} \times (\mathbf{H}_{\text{app}} + \alpha_{\text{ex}}\nabla^2\mathbf{M}) + \frac{\alpha_G}{M_s}\mathbf{M} \times \frac{d\mathbf{M}}{dt}, \quad (2)$$

where α_G is the Gilbert damping constant and $-\gamma$ is the electron gyromagnetic ratio. In the absence of external torques and damping the magnetization carries a magnetization current density

$$\tilde{\mathbf{j}}_\delta = \alpha_{\text{ex}}\mu_0\gamma\mathbf{M} \times \nabla_\delta\mathbf{M}, \quad (3)$$

which satisfies the continuity equation $d\mathbf{M}/dt + \nabla \cdot \tilde{\mathbf{j}} = 0$ [41]. When considering the excitation of magnetization, we include the microwave field $\mathbf{H}(t)$ in the LLG equation.

The microwaves emitted by a long stripline on top of a thin magnetic film launch a coherent magnon current normal to it. We consider a metallic wire of rectangular cross section $0 < x < d$ and $-w/2 < y < w/2$ (Fig. 1) with an AC current density I of frequency ω_s . The microwaves are uniform over the film thickness when $s \ll d$. The Fourier component k_y of the Oersted magnetic field in the thin film below the stripline ($x \rightarrow -s/2$) reads [27–29, 42–44],

$$\begin{aligned} H_x(k_y, \omega_s) &= (i/2)I(\omega_s)\mathcal{F}(d, w)\text{sgn}(k_y)e^{-|k_y|(d+s)/2}, \\ H_y(k_y, \omega_s) &= -(1/2)I(\omega_s)\mathcal{F}(d, w)e^{-|k_y|(d+s)/2}, \end{aligned} \quad (4)$$

with $\mathcal{F}(d, w) = (2/k_y^2)\sin(k_y w/2)(1 - e^{-|k_y|d})$ determined by stripline dimensions. Here we used $|k_y| \gg \omega_s/c$ because the velocity of light c is much larger than that of the magnons. The magnetic field $H_y(k_y, \omega_s) = i\text{sgn}(k_y)H_x(k_y, \omega_s)$ is right and left circularly polarized for positive and negative k_y , respectively, so polarization and momentum are locked. In the linear regime, this field coherently excites circularly-polarized magnons that propagate unidirectionally and populate at one side

of the stripline, i.e., a chiral pumping effect. This picture will be thoroughly changed in the nonlinear regime, however (see below).

Figure 2 illustrates the pumped magnon spin current $\mathbf{J}_y(y = 0) = -1/(2\omega_M\gamma\alpha_{\text{ex}})\int_{-s}^0 dx \tilde{\mathbf{j}}_y(x, y = 0)$ with $\omega_M \equiv \mu_0\gamma M_s$ as a function of the applied electric current density I with frequency $\omega_s \approx \{5.8, 11.3\}$ GHz across the stripline of width $w = \{150, 200\}$ nm and thickness $d = 80$ nm [8, 44] from numerical solutions of the LLG equation. Here the YIG film thickness $s = 10$ nm, the applied static magnetic field $\mu_0 H_{\text{app}} = 10$ mT that drives out domain walls [8, 40], $\mu_0 M_s = 0.18$ T, and $\alpha_G = 10^{-4}$. With the increase of the biased current in the stripline, the spin current firstly linearly increase but become saturated or maximal at a critical electric current I_c . This phenomenon is completely unexpected for non-interacting magnons that should scale as $|\mathbf{J}_y| \propto I^2$, which highlights the importance of the interaction effects discussed in the following.

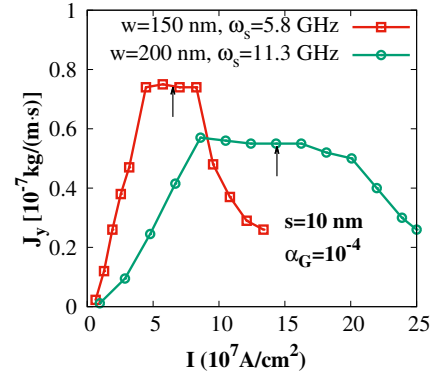


FIG. 2. (Color online) Maximum spin current excited in a magnetic film with thickness $s = 10$ nm by an AC charge current density I in a proximity microwave stripline calculated by numerically solving the LLG equation. The black arrows indicate the critical current density I_c for the indicated frequencies ω_s and stripline widths w .

Magnonic Doppler effect.—The LLG phenomenology contains all of the nonlinearities that can be captured by interacting magnons to some extent. The Holstein-Primakoff transformation expresses the magnetization dynamics by bosonic magnon operators $\hat{\Theta}(\mathbf{r})$ with $\hat{S}_x(\mathbf{r}) + i\hat{S}_y(\mathbf{r}) = \hat{\Theta}^\dagger(\mathbf{r})\sqrt{2S - \hat{\Theta}^\dagger(\mathbf{r})\hat{\Theta}(\mathbf{r})}$ and $\hat{S}_z(\mathbf{r}) = -S + \hat{\Theta}^\dagger(\mathbf{r})\hat{\Theta}(\mathbf{r})$, where the spin operators $\hat{\mathbf{S}} = -\mathbf{M}/(\gamma\hbar)$. The leading terms in the expansion of the square roots leads to a complete set of harmonic oscillators that we use to expand the full problem. The eigenmodes normal to the film plane depend on the boundary conditions that become free for thin films [45]. The magnon operators in position space can then be expanded in perpendicular standing spin waves (PSSWs) with in-

dex l [37, 38]

$$\hat{\Theta}(\mathbf{r}) = \sum_{l \geq 0} \sqrt{\frac{2}{1 + \delta_{l0}}} \frac{1}{\sqrt{s}} \cos\left(\frac{l\pi}{s}x\right) \hat{\Psi}_l(\boldsymbol{\rho}), \quad (5)$$

where $\boldsymbol{\rho} = y\hat{\mathbf{y}} + z\hat{\mathbf{z}}$. Substituting these expressions into the Holstein-Primakoff expansion, the Hamiltonian can be written as $\hat{H} = \hat{H}_L + \hat{H}_{NL} + \dots$, where \hat{H}_L describes the non-interacting magnon gas and \hat{H}_{NL} is the leading nonlinear term that introduces interactions between the magnons. At sufficiently low magnon densities

$$\hat{H} \rightarrow \hat{H}_L = \sum_l (E_l + \hbar\omega_M \alpha_{\text{ex}} k^2) \int \hat{\Psi}_l^\dagger(\boldsymbol{\rho}) \hat{\Psi}_l(\boldsymbol{\rho}) d\boldsymbol{\rho}, \quad (6)$$

where $E_l = \mu_0 \gamma \hbar H_{\text{app}} + \hbar\omega_M \alpha_{\text{ex}} (l\pi/s)^2$ is the edge of the l -th band. The nonlinear Hamiltonian

$$\begin{aligned} \hat{H}_{NL} = & \sum_{l_i} \mathcal{U}_{l_1 l_2 l_3 l_4} \int \hat{\Psi}_{l_1}^\dagger(\boldsymbol{\rho}) \hat{\Psi}_{l_2}^\dagger(\boldsymbol{\rho}) \hat{\Psi}_{l_3}(\boldsymbol{\rho}) \hat{\Psi}_{l_4}(\boldsymbol{\rho}) d\boldsymbol{\rho} \\ & + \sum_{l_i} \mathcal{V}_{l_1 l_2 l_3 l_4} \int \hat{\Psi}_{l_1}^\dagger(\boldsymbol{\rho}) \hat{\Psi}_{l_2}^\dagger(\boldsymbol{\rho}) \nabla_{\boldsymbol{\rho}} \hat{\Psi}_{l_3} \cdot \nabla_{\boldsymbol{\rho}} \hat{\Psi}_{l_4} d\boldsymbol{\rho} + \text{H.c.} \end{aligned}$$

contains two types of magnon-number conserving interactions derived in the Supplemental Material [46]. The potentials

$$\begin{aligned} \mathcal{U}_{l_1 l_2 l_3 l_4} &= \frac{\mu_0 \gamma^2 \hbar^2 \alpha_{\text{ex}} l_3 l_4 \pi^2 \mathcal{A}_{l_1 l_2 l_3 l_4}}{s^3 \sqrt{(1 + \delta_{l_1 0})(1 + \delta_{l_2 0})(1 + \delta_{l_3 0})(1 + \delta_{l_4 0})}}, \\ \mathcal{V}_{l_1 l_2 l_3 l_4} &= \frac{\mu_0 \gamma^2 \hbar^2 \alpha_{\text{ex}} \mathcal{B}_{l_1 l_2 l_3 l_4}}{s \sqrt{(1 + \delta_{l_1 0})(1 + \delta_{l_2 0})(1 + \delta_{l_3 0})(1 + \delta_{l_4 0})}}, \end{aligned}$$

are governed by magnon-mode overlap integrals

$$\begin{aligned} \mathcal{A}_{l_1 l_2 l_3 l_4} &= \frac{1}{s} \int_{-s}^0 dx \Pi_{i=1,2} \cos\left(\frac{l_i \pi}{s} x\right) \Pi_{j=3,4} \sin\left(\frac{l_j \pi}{s} x\right), \\ \mathcal{B}_{l_1 l_2 l_3 l_4} &= \frac{1}{s} \int_{-s}^0 dx \Pi_{i=1,2,3,4} \cos\left(\frac{l_i \pi}{s} x\right). \end{aligned}$$

When $l_1 = 0$, the scattering potentials obey selection rules $\mathcal{U}_{0l_2l_3l_4} \propto l_3l_4(\delta_{l_2+l_3,l_4} + \delta_{l_2+l_4,l_3} - \delta_{l_3+l_4,l_2})$ and $\mathcal{V}_{0l_2l_3l_4} \propto (\delta_{l_2+l_3,l_4} + \delta_{l_2+l_4,l_3} + \delta_{l_2+l_3+l_4,0} + \delta_{l_3+l_4,l_2})$. In the two-dimensional limit, $\mathcal{U}_{0000} = 0$ vanishes, but $\mathcal{V}_{0000} = \mathcal{V}_{00ll} = \mathcal{V}_0 = \mu_0 \gamma^2 \hbar^2 \alpha_{\text{ex}} / (4s)$ is large. The divergence for vanishing film thickness is an artifact of the continuum approximation that breaks down when s approaches unit cell dimensions.

We are interested in the effect of a magnon current on a low-frequency coherent excitation, i.e., at excitation frequency $\omega/(2\pi) \lesssim 1$ GHz, which allows us to set $l_1 = 0$. Using the above selection rules of the scattering potentials and energy conservation, we prove in the Supplemental Material [46] that the incoherent scattering of these *low-energy* magnons by those in all other bands is marginally small. The leading nonlinearities in the coherent magnon states thus reduce to a self-consistent mean-field problem [47, 48], in which the interaction renormalizes the energy dispersion but does not affect magnon

dephasing and lifetime. The coherent magnon amplitude in the lowest band obeys a Heisenberg equation of motion that is augmented by the Gilbert damping [46],

$$\begin{aligned} i\hbar(1 - i\alpha_G) \frac{\partial \langle \hat{\Psi}_0(\boldsymbol{\rho}) \rangle}{\partial t} &= E_0 \langle \hat{\Psi}_0(\boldsymbol{\rho}) \rangle - \hbar\omega_M \alpha_{\text{ex}} \nabla^2 \langle \hat{\Psi}_0(\boldsymbol{\rho}) \rangle \\ &+ \frac{8i}{\hbar} \sum_{l' \geq 0} \mathcal{V}_{00l'l'} \mathbf{J}_{l'}(\boldsymbol{\rho}) \cdot \nabla_{\boldsymbol{\rho}} \langle \hat{\Psi}_0(\boldsymbol{\rho}) \rangle + P_{\text{ex}}, \end{aligned} \quad (7)$$

where $\langle \dots \rangle$ represents an ensemble average,

$$\mathbf{J}_l(\boldsymbol{\rho}) = \frac{\hbar}{2i} \left(\langle \hat{\Psi}_l^\dagger(\boldsymbol{\rho}) \nabla_{\boldsymbol{\rho}} \hat{\Psi}_l(\boldsymbol{\rho}) \rangle - \langle \hat{\Psi}_l(\boldsymbol{\rho}) \nabla_{\boldsymbol{\rho}} \hat{\Psi}_l^\dagger(\boldsymbol{\rho}) \rangle \right) \quad (8)$$

is the magnon linear-momentum current density in sub-band l with contributions from both coherent and incoherent magnons, and P_{ex} is a microwaves excitation source that will be specified below. The (locally) uniform magnon current hence engages the gradient (or momentum) of the magnon amplitude $\nabla_{\boldsymbol{\rho}} \langle \hat{\Psi}_0 \rangle$ and tilts the magnon dispersion, which is an interaction-induced drag effect [30, 31].

The magnon momentum current density [Eq. (8)] is proportional to the magnon-number current density $\tilde{\mathbf{J}}_l$ defined by the continuity and Heisenberg equations for the non-interacting magnon Hamiltonian, since the exchange magnons have a constant mass $\hbar/(2\omega_M \alpha_{\text{ex}})$. The former is also a spin current since in the absence of anisotropies the magnons carry angular momentum \hbar . With magnon density operator $\hat{\rho}_m^l(\boldsymbol{\rho}) = \langle \hat{\Psi}_l^\dagger(\boldsymbol{\rho}) \hat{\Psi}_l(\boldsymbol{\rho}) \rangle$

$$\frac{\partial \hat{\rho}_m^l(\boldsymbol{\rho})}{\partial t} = \frac{1}{i\hbar} [\hat{\rho}_m^l(\boldsymbol{\rho}), \hat{H}_L] = -\nabla \cdot \tilde{\mathbf{J}}_l(\boldsymbol{\rho}), \quad (9)$$

leading to $\langle \tilde{\mathbf{J}}_l(\boldsymbol{\rho}) \rangle = (2\omega_M \alpha_{\text{ex}}/\hbar) \mathbf{J}_l(\boldsymbol{\rho})$, which is consistent with Eq. (3) since $-1/(\gamma\hbar) \int dx \tilde{\mathbf{j}}(x, \boldsymbol{\rho}) \rightarrow \tilde{\mathbf{J}}_l(\boldsymbol{\rho})$ when $l = 0$ to linear order in the magnon operator.

This stripline microwave field [Eq. (4)] couples to the magnons of the lowest PSSW band up to wave numbers $k_y \sim \pi/w$ by the Zeeman interaction

$$\hat{H}_Z = g \sum_{k_y} (H_x(k_y, t) - i \cos \varphi H_y(k_y, t)) \hat{\Psi}_0^\dagger(k_y) + \text{H.c.},$$

with coupling constant $g = \mu_0 \sqrt{\gamma \hbar M_s s/2}$, so the excitation source $P_{\text{ex}} = g(H_x(k_y, t) - i \cos \varphi H_y(k_y, t))$ in Eq. (7). The in-plane magnetization angle φ can be rotated by an applied DC magnetic field to tune the magnitude and direction of the pumped magnon current. When $\varphi = 0$, the stripline magnetic field launches a magnon current with $k_y > 0$ into half space (see below). Thereby the excited magnon current $\mathbf{J}_y(y > 0) = \tilde{\mathbf{J}}_y \exp(-y/\delta)$ decays exponentially with distance from the source on the scale of the decay length $\delta(\omega_s) \sim 2/\text{Im } \kappa_y \sim \sqrt{(\alpha_{\text{ex}} \omega_M)(\omega_s - \mu_0 \gamma H_{\text{app}})/(\alpha_G \omega_s)}$, i.e. the root of $(\omega_s - \mu_0 \gamma H_{\text{app}} - \omega_M \alpha_{\text{ex}} \kappa_y^2)^2 + (\alpha_G \omega_s)^2 = 0$. On

the other hand, the amplitude $\langle \hat{\Psi}_0(\rho) \rangle$ oscillates rapidly with wavelength ($1/|\kappa_y| \ll \delta$). Near the stripline, the magnon current in the lowest band obeys the integral equation, obtained from Eq. (7),

$$\bar{\mathbf{J}}_y = \frac{1}{\delta} \left(\frac{g}{\hbar} \right)^2 \int \frac{dk_y}{2\pi} k_y \frac{|H_x(k_y) - iH_y(k_y)|^2}{(\omega_s - \tilde{\omega}_{k_y})^2 + \alpha_G^2 \omega_s^2}, \quad (10)$$

with Doppler-shifted magnon frequency

$$\tilde{\omega}_{\mathbf{k}} = \mu_0 \gamma H_{\text{app}} + \omega_M \alpha_{\text{ex}} k^2 - (8/\hbar^2) \mathcal{V}_0 k_y \bar{\mathbf{J}}_y, \quad (11)$$

which can be solved iteratively or graphically.

Figure 3(a) illustrates the pumped magnon current $\bar{\mathbf{J}}_y$ as a function of the applied electric current density I with frequency $\omega_s/(2\pi) \approx 0.93$ GHz across the stripline of width $w = 150$ nm and thickness $d = 80$ nm [8, 44] from Eq. (10) in comparison with numerical solutions of the LLG equation [Eq. (3)]. Magnons of wavelength $2w$

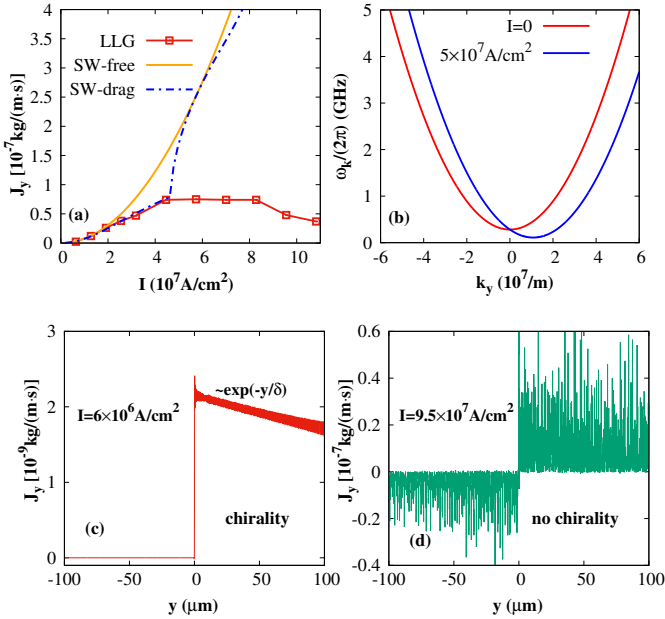


FIG. 3. (Color online) Magnon currents and Doppler shift of the magnon dispersion under stripline microwave excitation. (a) shows the coherently pumped magnon current $\bar{\mathbf{J}}_y$ in the stripline from numerical LLG calculations (“LLG”), non-interacting spin-wave theory (“SW-free”), and spin-wave theory including the drag effect (“SW-drag”). The tilt of the magnon dispersion at high excitation is illustrated in (b). We illustrate the chirality of the spin-current excitation for $I < I_c$ [(c)] and $I > I_c$ [(d)], respectively.

are resonantly excited and carry a current with decay length $\delta \approx 333 \mu\text{m}$. Here we compare the analytical solutions with the numerically exact solution of the LLG equation, which predicts a maximum spin-wave current for a stripline current $I_c \approx 5 \times 10^7 \text{ A}/\text{cm}^2$. The non-interacting spin-wave theory (SW-free) fails already for

small I , which emphasizes the importance of nonlinearities. When including the drag effect, the spin-wave theory Eq. (10) $\bar{\mathbf{J}}_y$ saturates at a current $I \sim I_c$, but returns to the non-interacting values at larger currents. When $I > I_c$, the lowest-order nonlinearity of the Holstein-Primakoff expansion and thereby the mean-field theory may break down. The Doppler shift of the spin-wave dispersion illustrated in Fig. 3(b) holds only for $I < I_c$. More detailed comparison with different parameters confirms these features [46]. When $I \gtrsim I_c$, we observe that the chirality of the magnon excitation is strongly reduced, indicating that the backscattering of magnons becomes strong, as illustrated by Figs. 4(c) and (d), which is partly responsible for the suppression of spin current.

I_c can be estimated by the onset of a spin-wave instability that is characterized by negative magnon excitation energy [23, 24, 26], which causes the discontinuous change of the spin current calculated by the mean-field theory. According to Eq. (11) a critical magnon current

$$\mathbf{J}_y^{(c)} = \hbar/(4\mathcal{V}_0) \sqrt{\hbar \omega_M \alpha_{\text{ex}} E_0} \quad (12)$$

can cause negative magnon excitation energies $\tilde{E}_0(\mathbf{k}) < 0$ at the momentum $k_y^{(c)} = 4\mathcal{V}_0 \bar{\mathbf{J}}_y / (\hbar^2 \omega_M \alpha_{\text{ex}})$. With the above YIG parameters, the critical magnon current $\mathbf{J}_y^{(c)} \approx 10^{-7} \text{ kg}/(\text{m} \cdot \text{s})$. This value can be reached by incoherent spin injection with a critical temperature gradient $4 \text{ K}/\mu\text{m}$ when $T = 300 \text{ K}$ [46]. However, according to the LLG calculations in Fig. 2 with different material parameters nonlinearities might prohibit reaching this critical value, which thus provides an upper limit in the estimation of maximal spin currents (more detailed comparison refers to the Supplemental Material [46]).

The tilt of dispersion causes chiral velocities of spin waves of the same energy that should be observable by changes in the microwave transmission [8, 40], nitrogen-vacancy center magnetometry [44, 49], and Brillouin light scattering [50]. The dispersion tilts into the opposite direction when the magnetization direction is reversed ($\varphi = \pi$) and vanishes when perpendicular to the stripline ($\varphi = \pi/2$), i.e., it follows the current direction governed by the chirality of the stripline magnetic field. The basic features agree with recently reported experiments in YIG thin films of thickness $s = 7 \text{ nm}$ [8] that were interpreted in terms of the DMI although spin-orbit interaction is small for closed-shell magnetic moments [51]. The Doppler effect, on the other hand, is tunable by the magnitude and direction of the excited magnonic spin current and does not require special interfaces. We note that an interfacial DMI causes additional shift of the magnon dispersion that favors the realization of spin-wave instability as calculated in the Supplemental Material [46].

Breaking of chiral pumping.—Finally, mean-field theory reveals a connection between the breakdown of the chiral pumping and the spin-wave instability. Around the critical driving strength I_c the magnon density on one

side of the stripline reaches its maximum with a rapid increase of the magnon density on the other side. Figure 4 shows the suppression of chirality under strong excitation. The nonequilibrium magnetization for $y > 0$ is largest around I_c , at which magnons accumulate also at $y < 0$. The chirality is strongly broken for larger drives, with nearly equal excited magnon densities on both sides of the stripline such that the injected power propagates into both directions, similar to the electric or thermal injection of an incoherent magnon accumulation.

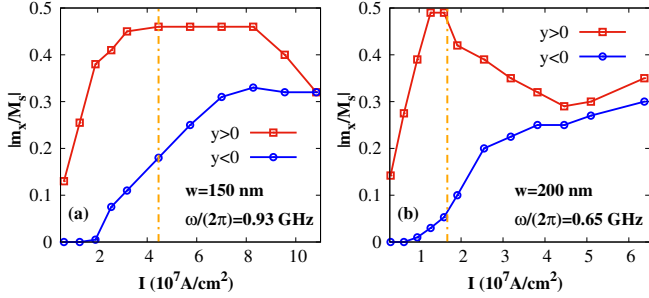


FIG. 4. (Color online) Magnon densities (reduced magnetization) at the right and left side of a stripline as a function of current density I with excitation frequencies $\omega_s = 2\pi \times 0.93 \text{ GHz}$, width $w = 150 \text{ nm}$ [(a)] and $2\pi \times 0.65 \text{ GHz}$, width $w = 200 \text{ nm}$ [(b)]. The vertical orange line indicates the critical I_c that maximizes the spin current.

Discussion.—In conclusion, we formulated the dynamics of a strongly driven ultrathin film of magnetic insulator such as YIG. We predict a Doppler shift of the magnon dispersion and a maximum spin current that a given sample can sustain. In our example, the effects should occur at stripline current densities $\sim 2 \times 10^7 \text{ A/cm}^2$ in one or $\sim (2/\mathcal{N}) \times 10^7 \text{ A/cm}^2$ in \mathcal{N} striplines (distributed over a total width that should be small compared to the magnon propagation length, i.e., many micrometers). The nonmonotonic dependence of the spin current excited by microwaves power may be related to the observed non-monotonicity of spin transport in magnon transistors as a function of gate-injected magnon densities [11, 17]. Our theory should help understanding the effects of large magnon spin currents on the magnetic order of insulators and provides a different scenario for the nonlinearities induced by the magnon chemical potential [13–16, 52–55].

This work is financially supported by DFG Emmy Noether program (SE 2558/2-1) as well as JSPS KAKENHI Grant No. 19H006450. C.W. is supported by the National Natural Science Foundation of China under Grant No. 11704061. We thank Xiang-Yang Wei, Hanchen Wang, Haiming Yu, and Mehrdad Elyasi for valuable discussions.

- [1] B. Lenk, H. Ulrichs, F. Garbs, and M. Muenzenberg, *Phys. Rep.* **507**, 107 (2011).
- [2] A. V. Chumak, V. I. Vasyuchka, A. A. Serga, and B. Hillebrands, *Nat. Phys.* **11**, 453 (2015).
- [3] D. Grundler, *Nat. Nanotechnol.* **11**, 407 (2016).
- [4] V. E. Demidov, S. Urazhdin, G. de Loubens, O. Klein, V. Cros, A. Anane, and S. O. Demokritov, *Phys. Rep.* **673**, 1 (2017).
- [5] A. Brataas, B. van Wees, O. Klein, G. de Loubens, and M. Viret, *Phys. Rep.* **885**, 1 (2020).
- [6] H. Chang, P. Li, W. Zhang, T. Liu, A. Hoffmann, L. Deng, and M. Wu, *IEEE Magn. Lett.* **5**, 6700104 (2014).
- [7] V. Cherepanov, I. Kolokolov, and V. L'vov, *Phys. Rep.* **229**, 81 (1993).
- [8] H. C. Wang, J. L. Chen, T. Liu, J. Y. Zhang, K. Baumgaertl, C. Y. Guo, Y. H. Li, C. P. Liu, P. Che, S. Tu, S. Liu, P. Gao, X. F. Han, D. P. Yu, M. Z. Wu, D. Grundler, and H. M. Yu, *Phys. Rev. Lett.* **124**, 027203 (2020).
- [9] J. Mendil, M. Trassin, Q. Bu, J. Schaab, M. Baumgartner, C. Murer, P. T. Dao, J. Vijayakumar, D. Bracher, C. Bouillet, C. A. F. Vaz, M. Fiebig, and P. Gambardella, *Phys. Rev. Mat.* **3**, 034403 (2019).
- [10] L. J. Cornelissen, J. Liu, B. J. van Wees, and R. A. Duine, *Phys. Rev. Lett.* **120**, 097702 (2018).
- [11] T. Wimmer, M. Althammer, L. Liensberger, N. Vlietstra, S. Geprägs, M. Weiler, R. Gross, and H. Huebl, *Phys. Rev. Lett.* **123**, 257201 (2019).
- [12] L. J. Cornelissen, K. J. H. Peters, G. E. W. Bauer, R. A. Duine, and B. J. van Wees, *Phys. Rev. B* **94**, 014412 (2016).
- [13] P. W. Anderson and H. Suhl, *Phys. Rev.* **100**, 1788 (1955).
- [14] V. S. L'vov, *Wave Turbulence Under Parametric Excitation* (Springer-Verlag Berlin Heidelberg, 1994).
- [15] S. O. Demokritov, V. E. Demidov, G. A. Melkov, A. A. Serga, B. Hillebrands, and A. N. Slavin, *Nature (London)* **443**, 430 (2006).
- [16] J. Liu, F. Feringa, B. Flebus, L. J. Cornelissen, J. C. Leutenantsmeyer, R. A. Duine, and B. J. van Wees, *Phys. Rev. B* **99**, 054420 (2019).
- [17] J. Liu, X.-Y. Wei, G. E. W. Bauer, J. Ben Youssef, and B. J. van Wees, arXiv:2011.07800.
- [18] P. Fulde, *Tunneling Phenomena in Solids* (Plenum, New York, 1969).
- [19] A. Kohen, Th. Proslier, T. Cren, Y. Noat, W. Sacks, H. Berger, and D. Roditchev, *Phys. Rev. Lett.* **97**, 027001 (2006).
- [20] T. Yu and M. W. Wu, *Phys. Rev. B* **94**, 205305 (2016).
- [21] S. Zhang and Z. Li, *Phys. Rev. Lett.* **93**, 127204 (2004).
- [22] Y. Tserkovnyak, H. J. Skadsem, A. Brataas, and G. E. W. Bauer, *Phys. Rev. B* **74**, 144405 (2006).
- [23] Ya. B. Bazaliy, B. A. Jones, and S.-C. Zhang, *Phys. Rev. B* **57**, R3213(R) (1998).
- [24] J. Fernández-Rossier, M. Braun, A. S. Núñez, and A. H. MacDonald, *Phys. Rev. B* **69**, 174412 (2004).
- [25] R. J. Doornenbal, A. Roldán-Molina, A. S. Nunez, and R. A. Duine, *Phys. Rev. Lett.* **122**, 037203 (2019).
- [26] J. Shibata, G. Tatara, and H. Kohno, *Phys. Rev. Lett.* **94**, 076601 (2005).
- [27] T. Schneider, A. A. Serga, T. Neumann, B. Hillebrands, and M. P. Kostylev, *Phys. Rev. B* **77**, 214411 (2008).

- [28] V. E. Demidov, M. P. Kostylev, K. Rott, P. Krzysteczko, G. Reiss, and S. O. Demokritov, *Appl. Phys. Lett.* **95**, 2509 (2009).
- [29] T. Yu and G. E. W. Bauer, in *Chirality, Magnetism, and Magnetoelectricity: Separate Phenomena and Joint Effects in Metamaterial Structures*, edited by E. Kamenetskii (Springer International Publishing, 2021).
- [30] A. V. Chumak, P. Dhagat, A. Jander, A. A. Serga, and B. Hillebrands, *Phys. Rev. B* **81**, 140404(R) (2010).
- [31] V. Vlaminck and M. Bailleul, *Science* **322**, 410 (2008).
- [32] I. A. Dzyaloshinsky, *J. Phys. Chem. Solids* **4**, 241 (1958).
- [33] T. Moriya, *Phys. Rev. Lett.* **4**, 228 (1960).
- [34] J.-H. Moon, S.-M. Seo, K.-J. Lee, K.-W. Kim, J. Ryu, H.-W. Lee, R. D. McMichael, and M. D. Stiles, *Phys. Rev. B* **88**, 184404 (2013).
- [35] T. Wolfram and R. E. De Wames, *Phys. Rev. Lett.* **24**, 1489 (1970).
- [36] B. A. Kalinikos, M. P. Kostylev, N. V. Kozhus, and A. N. Slavin, *J. Phys.:Condens. Matter* **2**, 9861 (1990).
- [37] C. Bayer, J. Jorzick, B. Hillebrands, S. O. Demokritov, R. Kouba, R. Bozinoski, A. N. Slavin, K. Y. Guslienkov, D. V. Berkov, N. L. Gorn, and M. P. Kostylev, *Phys. Rev. B* **72**, 064427 (2005).
- [38] T. Yu, C. P. Liu, H. M. Yu, Y. M. Blanter, and G. E. W. Bauer, *Phys. Rev. B* **99**, 134424 (2019).
- [39] S. Klingler, A. V. Chumak, T. Mewes, B. Khodadadi, C. Mewes, C. Dubs, O. Surzhenko, B. Hillebrands, and A. Conca, *J. Phys. D* **48**, 015001 (2015).
- [40] H. C. Wang, J. L. Chen, T. Yu, C. P. Liu, C. Y. Guo, H. Jia, S. Liu, K. Shen, T. Liu, J. Y. Zhang, M. A. Cabero Z, Q. M. Song, S. Tu, L. Flacke, M. Althammer, M. Weiler, M. Z. Wu, X. F. Han, K. Xia, D. P. Yu, G. E. W. Bauer, and H. M. Yu, *arXiv:2005.10452*.
- [41] Y. Tserkovnyak and M. Kläui, *Phys. Rev. Lett.* **119**, 187705 (2017).
- [42] J. D. Jackson, *Classical Electrodynamics* (Wiley, New York, 1998).
- [43] P. Lodahl, S. Mahmoodian, S. Stobbe, A. Rauschenbeutel, P. Schneeweiss, J. Volz, H. Pichler, and P. Zoller, *Nature (London)* **541**, 473 (2017).
- [44] I. Bertelli, J. J. Carmiggelt, T. Yu, B. G. Simon, C. C. Poethoven, G. E. W. Bauer, Y. M. Blanter, J. Aarts, and T. van der Sar, *Sci. Adv.* **6**, eabd3556 (2020).
- [45] Q. Wang, B. Heinz, R. Verba, M. Kewenig, P. Pirro, M. Schneider, T. Meyer, B. Lagel, C. Dubs, T. Bracher, and A. V. Chumak, *Phys. Rev. Lett.* **122**, 247202 (2019).
- [46] See Supplemental Material at [...] for the derivation of interaction Hamiltonian and incoherent exchange scattering, detailed comparison of spin currents with different parameters and discussion of the effects of interfacial DMI.
- [47] A. A. Abrikosov, L. P. Gorkov, and I. E. Dzyaloshinski, *Methods of Quantum Field Theory in Statistical Physics* (Prentice Hall, Englewood Cliffs, N. J., 1963).
- [48] A. Griffin, T. Nikuni, and E. Zaremba, *Bose-Condensed Gases at Finite Temperatures* (Cambridge University Press, Cambridge, England, 2009).
- [49] F. Casola, T. van der Sar, and A. Yacoby, *Nat. Rev. Mat.* **3**, 17088 (2018).
- [50] S. O. Demokritov, B. Hillebrands, and A. N. Slavin, *Phys. Rep.* **348**, 441 (2001).
- [51] L. Caretta, E. Rosenberg, F. Bütner, T. Fakhrol, P. Gargiani, M. Valvidares, Z. Chen, P. Reddy, D. A. Muller, C. A. Ross, and G. S. D. Beach, *Nat. Comm.* **11**, 1090 (2020).
- [52] S. A. Bender, R. A. Duine, A. Brataas, and Y. Tserkovnyak, *Phys. Rev. B* **90**, 094409 (2014).
- [53] B. Flebus, S. A. Bender, Y. Tserkovnyak, and R. A. Duine, *Phys. Rev. Lett.* **116**, 117201 (2016).
- [54] C. Du, T. V. der Sar, T. X. Zhou, P. Upadhyaya, F. Casola, H. Zhang, M. C. Onbasli, C. A. Ross, R. L. Walsworth, Y. Tserkovnyak, and A. Yacoby, *Science* **357**, 195 (2017).
- [55] C. Ulloa, A. Tomadin, J. Shan, M. Polini, B. J. van Wees, and R. A. Duine, *Phys. Rev. Lett.* **123**, 117203 (2019).